Journal of Southeast University (English Edition) Vol. 32, No. 1, pp. 85 - 92 Mar. 2016 ISSN 1003—7985

Discrete element modeling of migration and evolution rules of coarse aggregates in the static compaction process

Liu Weidong Gao Ying

(School of Transportation, Southeast University, Nanjing 210096, China)

Abstract: To investigate migration and evolution rules of coarse aggregates in the static compaction process, an algorithm of generating digital coarse aggregates that can reflect real morphology (such as shape, size and fracture surface) of aggregate particles, is represented by polyhedral particles based on the discrete element method (DEM). A digital specimen comprised of aggregates and air voids is developed. In addition, a static compaction model consisting of a digital specimen and three plates is constructed and a series of evaluation indices such as mean contact force σ_{MCF}, wall stress in direction of z-coordinate σ_{WSZZ}, porosity and coordination numbers are presented to investigate the motion rules of coarse aggregates at different compaction displacements of 7.5, 15 and 30 mm. The three-dimensional static compaction model is also verified with laboratory measurements. The results indicate that the compaction displacements are positively related to σ_{MCF} and σ_{WSZZ}, which increase gradually with the increase in iterative steps. When the compaction proceeds, the digital specimen porosity decreases, but the coordination number increases. The variation ranges of these four indices are different at different compaction displacements. This study provides a method to analyze the compaction mechanism of particle materials such as asphalt mixture and graded broken stone.

Key words: asphalt mixture; coarse aggregate; static compaction; discrete element model

DOI: 10.3969/j.issn.1003 - 7985.2016.01.015

Asphalt mixture can be regarded as a multiphase composite material consisting of asphalt mastic (fine aggregates, fines and asphalt binder), coarse aggregates and air voids[1]. For the asphalt binder, both high temperature softening and cold hardening properties are sensitive to temperature. The loose and hot asphalt mixture shows a plasticity-viscoelasticity characteristic during compaction. Based on the Burgers rheological model, the creep deformation and relaxation behavior can be used to describe the viscoelasticity behavior of asphalt mixture. The constitutive model of hot asphalt mixture and the corresponding parameters are investigated through a large number of laboratory measurements during the compaction process[2-3].

The mineral aggregate of asphalt mixture constitution by volume and weight is approximately 85% and 95%, respectively[1]. The asphalt mixture mechanical properties are significantly related to the morphological characteristics, such as sphericity, fractured face, texture and size, orientation, and the volume of coarse aggregates[4-6]. The morphological features of coarse aggregate are determined based on the regular methods including image-based and X-ray CT (computed tomography). Apparently, they are reliable and persuasive. However, the integrity of asphalt mixture is damaged by a destructive cutting way. In addition, a small number of asphalt mixture specimens with heterogeneous multiphase composites are utilized to investigate the mechanical response; the variability of experimental results is significant. Laboratory testing approaches on asphalt mixture are time-consuming, laborious and expensive. The two-dimensional image-based model is limited in obtaining the precise interlock effect and contacts between aggregate particles in the three-dimensional field. Furthermore, these two-dimensional image-based models are greatly dependent on digital image processing (DIP) and raw materials. In particular, a large number of specimens need to be prepared[7].

The skeleton structure of coarse aggregates, which is almost unaffected by temperature, is one of the main components of asphalt mixture strength. Effects of coarse aggregates and air voids on asphalt mixtures viscoelasticity were investigated from micromechanics analysis[8]. Based upon DIP technology, the indices including the number of aggregate-to-aggregate proximity zone, total proximity zone length and proximity zone plane orientation are used to characterize the coarse aggregates structure. The results indicate that these indices are correlated with the asphalt mixture properties[9].

Due to the friendly interfaces and numerous advantageous characteristics for simulation granular materials, the developed commercial DEM codes comprising of two-dimensional and three-dimensional particle flow codes (PFC2D and PFC3D) are widely utilized in most published studies. An open source code named YADE is used to simulate the SGC fabricating asphalt mixtures[10]. The

Received 2015-08-02.

Biographies: Liu Weidong (1985—), male, graduate; Gao Ying (corresponding author), female, doctor, associate professor, gy@seu.edu.cn.

Foundation item: The National Natural Science Foundation of China (No. 51108081).

Citation: Liu Weidong, Gao Ying. Discrete element modeling of migration and evolution rules of coarse aggregates in the static compaction process[J]. Journal of Southeast University (English Edition), 2016, 32(1): 85 - 92. DOI: 10.3969/j.issn.1003 - 7985.2016.01.015.

sizes and angularity of the coarse aggregates can be modeled well, but the morphology is not precisely related to the real aggregates[11]. Some algorithms for generating irregular particles with angularity and surface texture properties are investigated by using overlapping balls[12-14]. The coarse aggregates represented by polyhedral particles are developed. In this algorithm, the characteristics of aggregates are partially embodied, but the gradation and volume of asphalt mixture are in poor agreement with the actual aggregates[15]. A flexible algorithm for the generation of arbitrary-shaped aggregate grains is presented using the DEM approach, but this method is highly dependent on the image-based technology, which is time-consuming and requires sophisticated equipment[16].

The previous studies on DEM mainly focused on discussing the correlation between the macroscopic response of mechanical behavior and microstructure for the asphalt mixture[1,4,10]. The compaction process is a critical step for either field construction or experimental tests of asphalt mixtures. Most researchers focused on investigating the different compaction methods of asphalt mixture, such as superpave gyratory compaction (SGC), static and dynamic compaction from macroscopic analysis, but little literature reported on simulation compaction based on DEM. The main reasons can be assumed as follows: 1) The compaction behavior is very cumbersome based on current PFC3D, particularly, dynamic and SGC compaction; 2) The loose and hot asphalt mixture reveals a plasticity-viscoelasticity property, and the existing constitutive models cannot explain this complex behavior. Namely, a new constitutive model will be developed, and a series of microparameters needs to be calibrated. All these steps are highly time-consuming and difficult. However, if the asphalt binder and complicated compaction methods are not taken into consideration, the compaction process of the aggregate specimen can be achieved based on PFC3D. It should be noted that fine aggregates cannot form the skeleton structure, instead of increasing contacts between aggregates, and a large number of fine aggregates significantly limits computer capacity and efficiency. Therefore, in this paper, virtual specimens comprised of coarse aggregates and air voids are employed to conduct the static compaction based on PFC3D.

The major objective of this study is to develop a static compaction model for discussing the motion rules of coarse aggregates at different compaction displacements based on DEM. Coarse aggregates represented by irregular polyhedrons were developed, according to truncating the graded spheres with the randomly created cutting planes. The static compaction model of the aggregates specimen was established to analyze the effects of different compaction displacements of 7.5, 15 and 30 mm on the motion rules of coarse aggregates. In addition, these evaluation indices, such as σ_{MCF}, σ_{WSZZ}, porosity, and coordination number were used to investigate the migration and evolution of coarse aggregates.

1 Digital Aggregate Generation

As shown in Fig. 1, R and $O(x_0, y_0, z_0)$ are the radius and center of a graded ball, respectively; d is the distance between the cutting planes and the center of the graded ball.

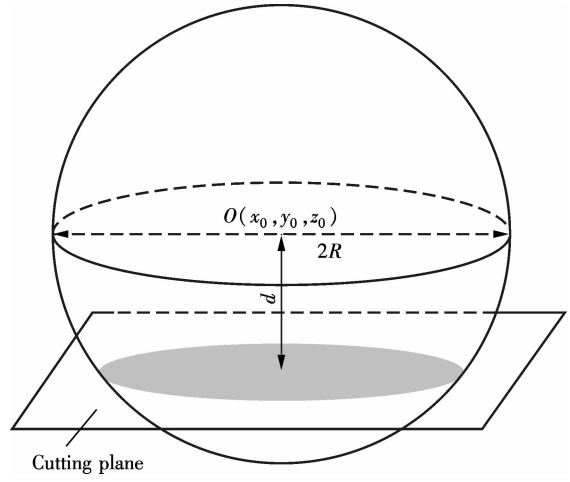

Fig. 1 Algorithm for creating a polyhedral particle

The generation of a coarse aggregate is presented based on Ref. [1].

$$(x-x_0)^2+(y-y_0)^2+(z-z_0)^2\leqslant R^2 \tag{1}$$

$$n_x=\cos(2\pi U),\ n_y=\cos(2\pi U),\ n_z=\cos(2\pi U)$$
$$n_x(x-x_0)+n_y(y-y_0)+n_z(z-z_0)=0 \tag{2}$$

The critical discrepancy is that the polyhedron is created by manipulating the magnitude of d, instead of manipulating cut ratios. k is computed by $k=R/d$; $k_{\min}$ and $k_{\max}$ are the minimum and maximum values of k, respectively; $d_{\min}$ and $d_{\max}$ are the minimum and maximum values of the short axis length, respectively, and they can be obtained by Ref. [17]; U is a random-number generator, and its value ranges from 0 to 1.0.

$$\left.\begin{aligned} d_{\max}&=\frac{R}{k_{\min}}\\ d_{\min}&=\frac{R}{k_{\max}}\\ d&=d_{\min}+(d_{\max}-d_{\min})U\end{aligned}\right\} \tag{3}$$

The realistic morphology of the coarse aggregates including angularity, size, and shape can be described using this algorithm. The random distribution functions and aggregate gradation are used to express shapes and sizes. The setting of several cutting planes can control the fractured surfaces. As shown in Fig. 2, coarse aggregates are produced, and the diameter of the small-sized particles is 1 mm. However, the volume of the virtual aggregate particles is truncated by the cutting plane, and filled

with the small-sized particles, which does not represent the actual aggregates. It is necessary to check the volume of the aggregates by increasing their number according to the given gradation. After repeated attempts, adhering to the condition of not changing the gradation, the volume of the virtual aggregate is consistent with the real aggregate.

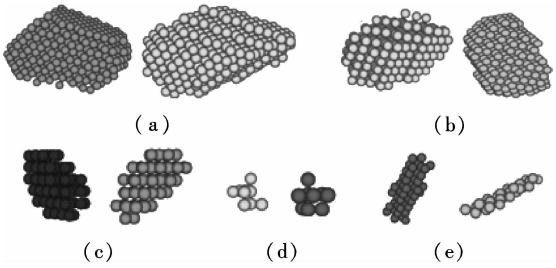

Fig. 2 Coarse aggregate particles. (a) 13.2 to 16 mm; (b) 9.5 to 13.2 mm; (c) 4.75 to 9.5 mm; (d) 2.36 to 4.75 mm; (e) Flat and elongate particles

2 Static Compaction Models

2.1 A virtual specimen generation

The virtual experiment on simulation of asphalt mixture mechanical behavior is conducted based upon DEM. The aggregate particles with sizes less than 2.36 mm have a secondary effect on skeleton structure and greatly limit computer capacity and efficiency. Therefore, the asphalt mixture can be regarded as three-phase composites of asphalt mastic (fine aggregates, fines and asphalt binder), coarse aggregates and air voids[1, 10–11, 14, 17]. In this study, since the hot asphalt mastic shows a complicated plasticity-viscoelasticity property which cannot be characterized by the current constitutive models, a virtual specimen consisting of coarse aggregates and air voids will be developed.

The generation of a digital specimen is shortly described as follows. The number of coarse aggregates can be calculated by a given coarse aggregate gradation, as shown in Tab. 1. Then, these coarse aggregates are inputted into a cylinder with a diameter of 100 mm and a height of 150 mm, and the overlaps between aggregate particles are eliminated by a user-defined program coded with FISH language. The graded balls are shown in Fig. 3 (a). In addition, the developed cylinder is filled with small-sized discrete particles. This assemblage action is a regular method, in which each small-sized particle has six identical particles except the boundary particles, as shown in Fig. 3(b). Based on the mentioned algorithm of aggregates, the graded balls are truncated. However, due to the rigid balls in PFC3D, it should be noted that this virtual truncating action is to save physical information. These small-sized particles are bonded together to represent a digital coarse aggregate so-called a "clump". Repeat the above steps until all of these graded balls are represented by the discrete particles. After checking the target gradation and volume of virtual aggregates, and deleting the remaining small-sized particles not belonging to any coarse aggregates, a two-phase system of coarse aggregates specimen is established, as shown in Fig. 3(c).

Tab. 1 Gradations of aggregate mixture

Sieve size/mm	Percentage passing/%
16	100
13.2	95
9.5	65
4.75	30
2.36	21
1.18	19
0.6	16
0.3	13
0.15	12
0.075	10

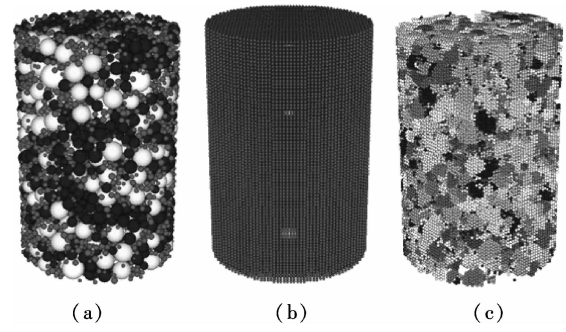

Fig. 3 A typical digital specimen. (a) Graded balls; (b) Regular array of small-sized discrete particles; (c) Two-phase digital specimen including coarse aggregates and air voids

2.2 Developing a static compaction model

Since the asphalt mastic is not considered, without cohesive force exhibiting between the coarse aggregate particles within the digital specimen, a numerical simulation of the digital specimen at a static compaction cannot be achieved under the unconfined constraints. Therefore, it is necessary to use a lateral plate as a boundary, as shown in Fig. 4. It should be noted that the interaction between walls cannot occur. The particles that have a considerable contact force during the loading period will escape and extrude. To solve this problem, the wall size should be slightly larger than that of the corresponding digital specimen. The platen stiffnesses should be large enough to ensure not to produce deformation, and their suggested value is 10 GN/m[18]. As shown in Fig. 4, a static compaction of the digital specimen is developed based on the upper loading plate moving down at a suitable velocity. Meanwhile, the bottom wall is fixed. It is significant to select an appropriate loading rate. During the static compaction test, the loading rate must be slow enough to ensure that the digital specimen remains in quasi-static equilibrium throughout the test, such that no inertial effects occur. The precise loading rate can be validated by the

stopping test and we can observe the load level at the upper plate. A constant load is obtained, which implies that the selective loading rate is reasonable[19]. However, there is no doubt that the slower the loading rate, the lower the computer efficiency. Therefore, the loading rate can properly increase under the principle of not changing the quasi-static equilibrium of the compaction model. The final loading rate, namely 0.15 mm/s, is confirmed based on the repeated trials.

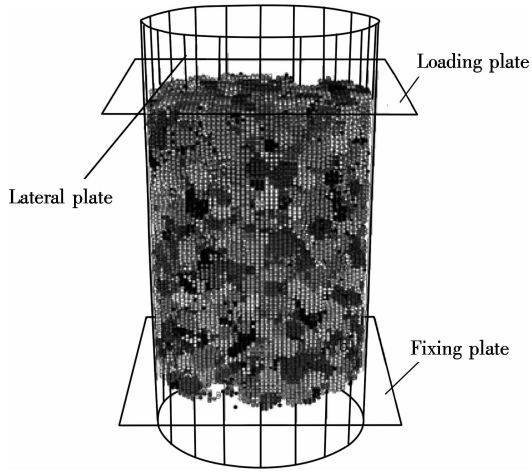

Fig. 4 A static compaction model of a digital specimen

In the compaction model, there are two different types of contacts: contacts within coarse aggregates and contacts between coarse aggregates. The coarse aggregate is regarded as a pure elastic material. The linear contact model and contact-bond model are used to represent the interactions within the coarse aggregates[18]. The linear contact model and the slip model are employed to represent the interactions between adjacent coarse aggregates. Based on the proposed compaction model using DEM, the contact stiffness of the aggregate particles can be expressed as[4, 11, 17-18]

$$k_n = 4Er, \quad k_s = \frac{2Er}{1+\upsilon} \tag{4}$$

where E is the Young's modulus at each particle-particle contact, and its value ranges from 30 to 85 GPa[20]; k_n and k_s are the normal and shear stiffness of the two contacting entities, respectively; υ is the Poisson's ratio, and its value is set to be 0.25[21]; r is the radius of the particle.

However, due to the complex relationship between the microparameters and microparameters, the numerical simulation results are usually not consistent with the experimental results according to the equation stated above. It should be noted that the equation only provides a reference range, but a precise stiffness can be determined using an approach called "inverse modeling". In this paper, a series of digital specimens are prepared for simulating trial microparameters and then these simulation results are compared with the laboratory results. While a good agreement is found, the appropriate parameters can be utilized in the model.

This paper aims to investigate the motion rules of coarse aggregates during the compaction process. The breakage of aggregates is suppressed by utilizing a remarkable bond strength. The correlations between migration and evolution of coarse aggregates and different compaction displacements are close. For the same mass fraction of aggregates, the greater the compaction displacement, the lower the air voids. It indicates that the number of overlap between particles is large. Accordingly, the contact force is considerable. Therefore, different compaction displacements including 7.5, 15 and 30 mm are selected to investigate the motion rules of coarse aggregates in the following simulations.

3 Simulation Results and Discussion

Mean contact force σ_{WSZZ} is defined as the average unbalanced force for the loading and fixing plates divided by the average area of two plates. Wall stress in the direction of the z-coordinate, σ_{MCF}, is defined as the contact force within coarse aggregates divided by the number of contacts. σ_{MCF} increases with the increase in loading time and compaction displacements are related to σ_{WSZZ} and σ_{MCF}, as shown in Figs. 5(a), (b) and (c). However, the effects of different compaction displacements on σ_{WSZZ} and σ_{MCF} are different. When the compaction displacements are 7.5, 15 and 30 mm, σ_{MCF} are 15, 46 and 120 N, and σ_{WSZZ} are 0.43, 2, and 8.1 MPa, respectively.

The coordinate number (CN) is the average number of contacts for each aggregate. The distribution of the measure spheres is shown in Fig. 6. The measure spheres' diameter of 30 mm is twice the maximum nominal size of the aggregates. The variability of aggregates, which are adjacent to the plates, cannot be overlooked. Therefore, the distances between the measure spheres and the lateral and fixing plate are 5 and 10 mm, respectively. In addition, the number of compaction displacements can affect the measure sphere layouts. The upper measure spheres are usually far away from the loading plate. Due to the complex distribution of the aggregates, the porosity and CN variability exhibit consequentially. The measure spheres are installed in all directions. The porosity and CN are the average of all the measure spheres monitoring the corresponding parameters.

With the increase in loading steps, the porosity of specimens decreases. On the contrary, the CN increases, as shown in Figs. 7(a), (b) and (c). The variation ranges of air voids and CN are different at different compaction displacements. When the compaction displacements of the virtual specimens are 7.5, 15 and 30 mm, the variation coefficients of the air voids are 3.3%, 5.2% and 10%, respectively. Meanwhile, the variation coefficients of CN are 2.63, 3.25 and 7.42, respectively.

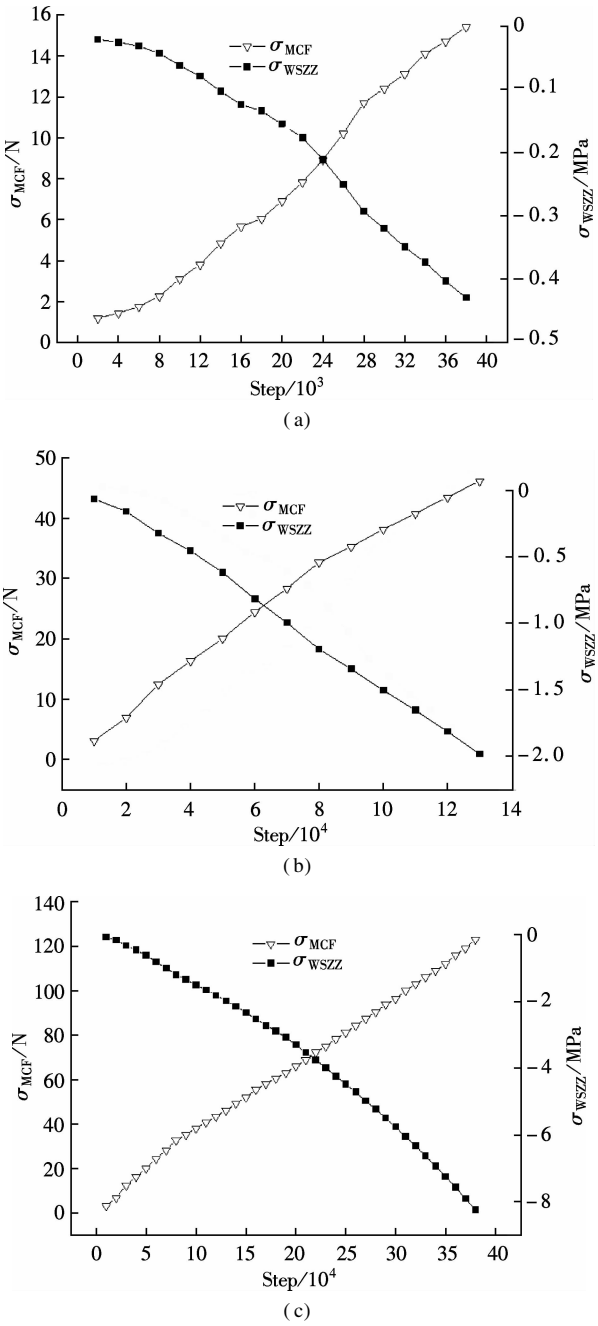

Fig. 5 σ_{WSZZ} and σ_{MCF} vs. loading steps at different compaction displacements. (a) 7.5 mm; (b) 15 mm; (c) 30 mm

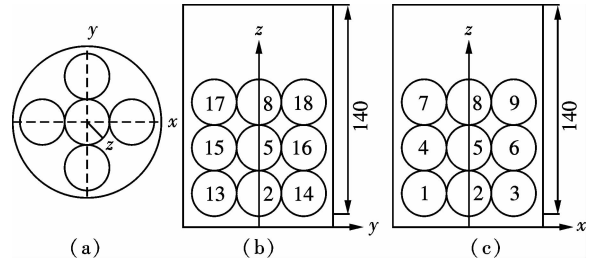

Fig. 6 Layouts of measure balls (unit: mm). (a) Top-view; (b) Sectional view of *yz*-plane; (c) Sectional view of *xz*-plane

The CN and σ_{MCF} that cannot be obtained using conventional laboratory experiments are used to characterize the motion rules of the aggregates from the microscopic

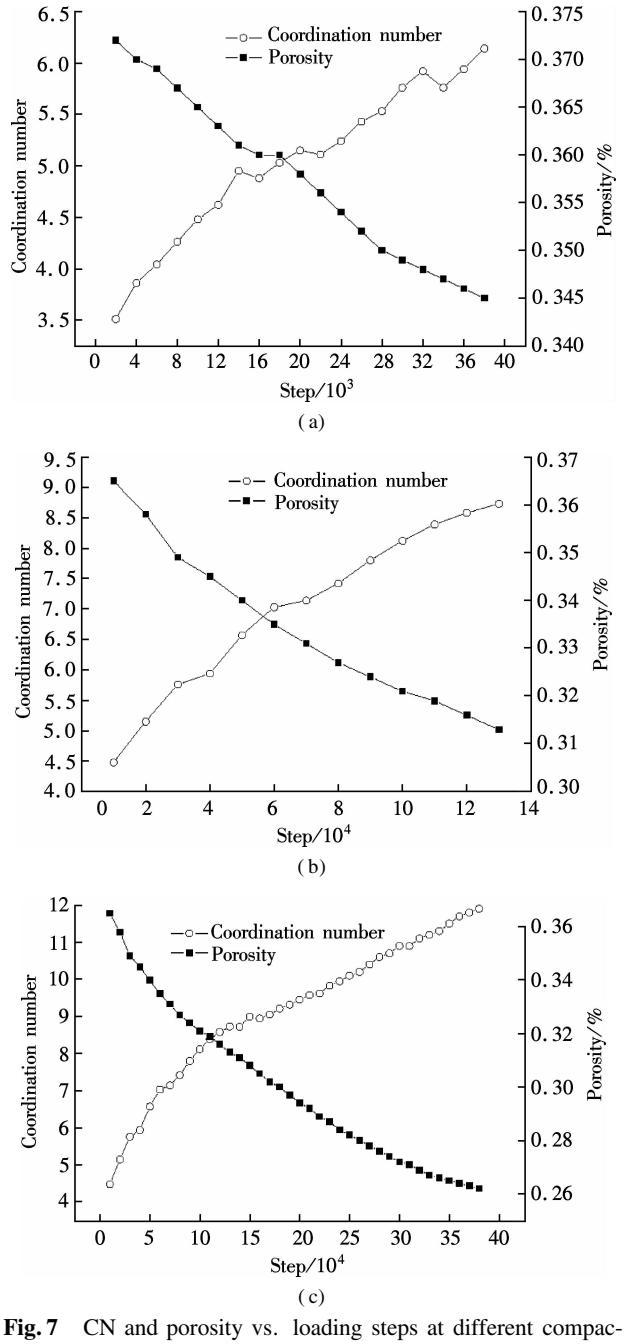

Fig. 7 CN and porosity vs. loading steps at different compaction displacements. (a) 7.5 mm; (b) 15 mm; (c) 30 mm

view. However, the porosity and σ_{WSZZ} are the macroscopic properties of aggregate actions. As shown in Fig. 8, the magnitude of contact force is proportional to the line width. The cohesive force does not exist between aggregates, namely, the aggregates cannot bear tensile stress. There is only compressive stress between aggregates. As discussed above, the reasons for the variation ranges of σ_{MCF} and σ_{WSZZ} greater than these of compaction displacements can be illustrated as follows. The initial porosity of the coarse aggregates specimen is large. Based on a low level of compaction displacement (such as 7.5 mm), the air voids decreases slightly. Consequently, the interlock effect of the aggregates is enhanced by the aggregate particles co-squeezing and embedding. Ultimate-

ly, the CN, σ_{WSZZ} and σ_{MCF} increase marginally. Fig. 7 (a), Figs. 8(a) and (b) reveal that σ_{MCF} and the maximum contact force $(\sigma_{CF})_{max}$ are less than 10 and 200 N, respectively, at the compaction displacement of 7.5 mm. The aggregate specimen volume decreases with the compaction displacement increasing. Meanwhile, the distance between the aggregates diminishes gradually. Therefore, a strong and powerful interlock effect of coarse aggregates is formed, and the magnitude of the coordinate number increases dramatically. Fig. 7(b), Figs. 8(c) and (d) indicate that σ_{MCF} and $(\sigma_{CF})_{max}$ approximate 25 and 550 N, respectively, at the compaction displacement of 15 mm where σ_{MCF} is twice that of the compaction displacement of 7.5 mm. To reach the given compaction displacement, σ_{WSZZ} needs to be augmented to overcome the skeletal effect. As shown in Figs. 8(e) and (f), the maximum contact force is greater than 1 000 N at the compaction displacement of 30 mm. The variation ranges of porosity and CN are larger in the high-level compaction displacement than those of the low-level compaction displacement.

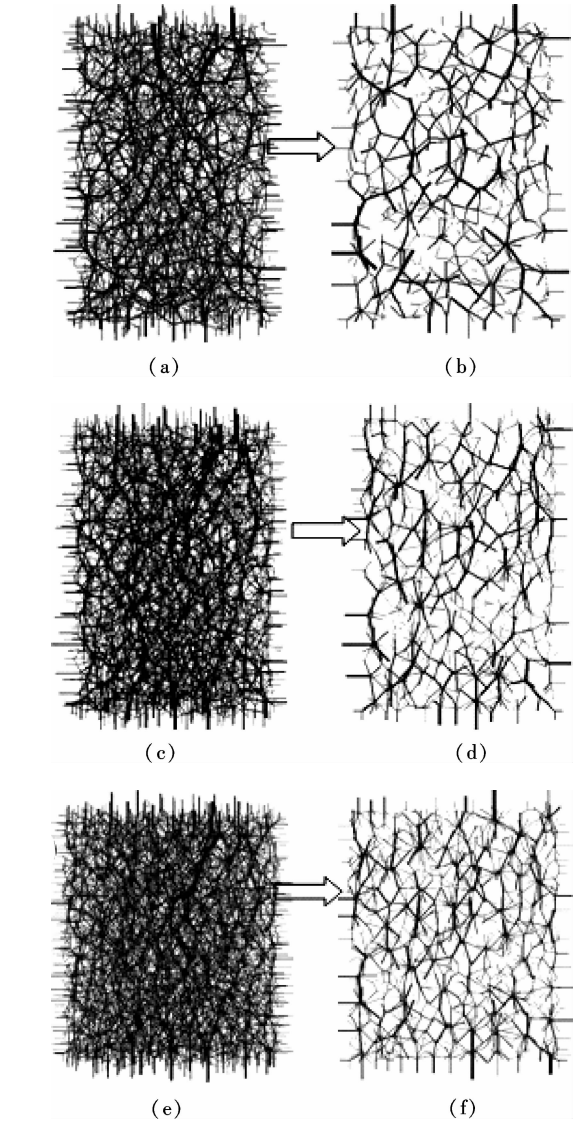

Fig. 8 Contact-force distribution at different compaction displacements. (a) 7.5 mm overall sketch, σ_{CF} = 195.4 N; (b) 7.5 mm vertical profile, σ_{CF} = 125.5 N; (c) 15 mm overall sketch, σ_{CF} = 548.4 N; (d) 15 mm vertical profile, σ_{CF} = 352 N; (e) 30 mm overall sketch, σ_{CF} = 1 587 N; (f) 30 mm vertical profile, σ_{CF} = 1 113 N

4 Validation of Compaction Model

An aggregate particle is a typical particulate matter. Based on the current experimental instruments, it is difficult to directly validate the microscopic indices of aggregates, such as the force chain and the coordinate number in the static compaction. In this study, the macroscopic indices including σ_{WSZZ} and porosity are used to verify the developed static compaction. Due to the uncrushable aggregates in the simulations, basalt with a great compressive strength is utilized in the validation tests. The basalt coarse aggregates with 2.88 g/cm^3 apparent specific gravity are first prepared according to the given gradation in Tab. 1. The cylinder mould sizes with the diameter of 100 mm and the height of 150 mm equal the digital specimen sizes. Then the prepared aggregates are packed into the container three times. It should be noted that the number of aggregates is roughly identical each time. In addition, after accomplishing each layer, the installed aggregates are densified using a metal bar inserted 25 times. When the aggregates specimen is fabricated, a critical step is to calibrate its volume fraction. If the porosity of the actual specimen is close to the given value of digital specimen, it suggests that the fabricated specimen is favorable. The favorable specimen is tested at the same 0.15 mm/s constant velocity as the digital specimen, which shows that the compaction approach is a static compaction. The cumulative compaction displacement is regarded as a controlling index[22]. The above experimental test was repeated three times. Fig. 9 shows the average simulation and experiment σ_{WSZZ} vs. compaction displacement. The simulation result is consistent with the experimental result, particularly for the low-level compaction displacement. It proves that the developed static compaction model is reliable and feasible.

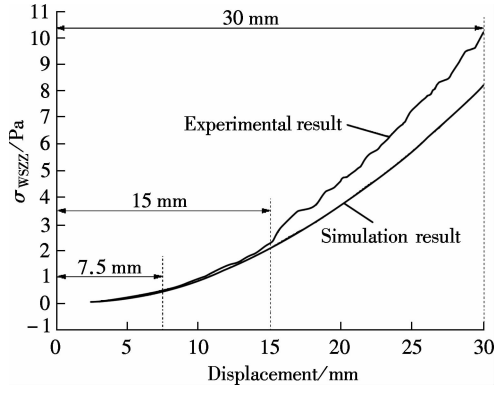

Fig. 9 σ_{WSZZ} vs. loading steps

In order to further verify the accuracy of the simulation, based on the aforementioned experiment, the porosity of the actual specimens is compared with the simulation porosity. The coarse aggregates mass, apparent density and cylinder mould volume which can be obtained in the experimental test. According to Ref. [23], the porosity can be calculated, as shown in Tab. 2. It can be found that simulation results are consistent with laboratory results. It indicates that the established static compaction model of coarse aggregates is reasonable.

Tab. 2 Porosity of laboratory test and simulation

Displacement/mm	Porosity		Error/%
	Laboratory results	Simulation results	
7.5	0.362	0.345	5
15	0.338	0.313	8
30	0.288	0.262	10

5 Conclusions

1) The evaluation indicators including σ_{WSZZ}, σ_{MCF}, porosity and CN are available to describe the motion rules of coarse aggregates during the static compaction.

2) σ_{WSZZ} and σ_{MCF} increase with the increase in loading steps. The compaction displacements are positively related to σ_{WSZZ} and σ_{MCF}. Nevertheless, their variation ranges are not similar at different compaction displacements. Within a certain scope of compaction displacement, the number of air voids decreases with the increase in loading steps, but the CN increases.

3) Based on the experimental results, a good agreement is found between the simulations and experimental tests. It shows that the developed static compaction model can be utilized as an effective assistant tool to investigate the microscopic mechanics of particulate matter, e.g., sandy soil and graded crushable rock, and particle-reinforced composites materials such as asphalt mixture and Portland cement concrete.

References

[1] Liu Y, You Z P. Visualization and simulation of asphalt concrete with randomly generated three-dimension models [J]. *Journal of Computing in Civil Engineering*, 2009, **23**(6): 340 − 347.

[2] Zheng J L, Chen X, Qian G P. Compaction mechanical response and analysis of viscoelastic-plasticity model parameter for loose hot asphalt mixture [J]. *Engineering Mechanics*, 2010, **27**(1): 33 − 40. (in Chinese)

[3] Chen X, Ying R H, Zheng J L, et al. Viscoelastic-plasticity model of hot asphalt mixtures based on MTS compaction test [J]. *China Journal of Highway and Transport*, 2007, **20**(6): 25 − 30. (in Chinese)

[4] Liu Y, You Z P. Discrete-element modeling: impacts of aggregate sphericity, orientation, and angularity on creep stiffness of idealized asphalt mixtures [J]. *Journal of Engineering Mechanics*, 2010, **137**(4): 294 − 303. DOI: 10.1061/(ASCE)EM.1943-7889.0000228.

[5] Pan T Y, Tutumluer E, Carpenter S H. Effect of coarse aggregate morphology on permanent deformation behavior of hot mix asphalt [J]. *Journal of Transportation Engineering*, 2006, **132**(7): 580 − 589. DOI: 10.1061/(ASCE)0733-947X(2006)132:7(580).

[6] Pan T, Tutumluer E, Carpenter S H. Effect of coarse aggregate morphology on the resilient modulus of hot-mix asphalt [J]. *Transportation Research Record*, 2005, **1929**: 1 − 9.

[7] Liu Y, You Z P, Li L, et al. Review on advances in modeling and simulation of stone-based paving materials [J]. *Construction and Building Materials*, 2013, **43**: 408 − 417.

[8] Huang X M, Li H G, Zhang Y Q. Micromechanics analysis of viscoelasticity for asphalt mixtures considering influences of coarse aggregates and voids [J]. *Journal of South China University of Technology* (*Natural Science Edition*), 2009, **37**(7): 31 − 36. (in Chinese)

[9] Sefidmazgi N R, Bahia H U. Effect of compaction conditions on aggregate packing using 2-dimensional image analysis and the relation to performance of HMA [J]. *Materials and Structures*, 2014, **47**(8): 1313 − 1324. DOI: 10.1617/s11527-014-0275-x.

[10] Chen J S, Huang B S, Chen F, et al. Application of discrete element method to Superpave gyratory compaction [J]. *Road Materials and Pavement Design*, 2012, **13**(3): 480 − 500. DOI: 10.1080/14680629.2012.694160.

[11] Zhang D, Huang X M, Zhao Y L. Algorithms for generating three-dimensional aggregates and asphalt mixture samples by the discrete-element method [J]. *Journal of Computing in Civil Engineering*, 2012, **27**(2): 111 − 117. DOI: 10.1061/(ASCE)CP.1943-5487.0000210.

[12] Lu M, McDowell G R. The importance of modelling ballast particle shape in the discrete element method [J]. *Granular Matter*, 2007, **9**(1/2): 69 − 80. DOI: 10.1007/s10035-006-0021-3.

[13] Garcia X, Latham J P, Xiang J, et al. A clustered overlapping sphere algorithm to represent real particles in discrete element modelling [J]. *Geotechnique*, 2009, **59**(9): 779 − 784. DOI: 10.1680/geot.8.T.037.

[14] Yang J, Wang K L. Virtual triaxial test simulation based on discrete element method for shear resistance property assessment of asphalt mixtures [J]. *Journal of Testing and Evaluation*, 2012, **40**(7): 1103 − 1111.

[15] Tian L, Liu Y, Hu X G, et al. Random generation algorithm for simulation of polyhedral particles in asphalt mixture aggregate and its program [J]. *China Journal of Highway and Transport*, 2007, **20**(3): 5 − 10. (in Chinese)

[16] He H, Guo Z, Stroeven P, et al. Characterization of the packing of aggregate in concrete by a discrete element approach [J]. *Materials Characterization*, 2009, **60**(10): 1082 − 1087. DOI: 10.1016/j.matchar.2009.02.012.

[17] Zhang D. Research on morphology of coarse aggregates and its mechanical performance by discrete element modeling [D]. Nanjing: School of Transportation, Southeast University, 2013. (in Chinese)

[18] Zhang D Y, Huang X M, Gao Y. Virtual rutting test of asphalt mixture using discrete element method[J]. *Journal of Southeast University* (*English Edition*), 2012, **28**(2):

215 – 220.
[19] Abbas, A R. Simulating the deformation behavior of hot mix asphalt in the indirect tension test[C]//*Symposium on Pavement Mechanics and Materials*. Blacksburg, VA, USA, 2008: 16 – 23.
[20] Dai Q L, You Z P. Prediction of creep stiffness of asphalt mixture with micromechanical finite-element and discrete-element models[J]. *Journal of Engineering Mechanics*, 2007, **133**(2): 163 – 173.
[21] You Z P, Buttlar W G. Discrete element modeling to predict the modulus of asphalt concrete mixtures [J]. *Journal of Materials in Civil Engineering*, 2004, **16**(2): 140 – 146.
[22] Ministry of Communications of the People's Republic of China. JTG E20—2011 Standard test methods of bitumen and bituminous mixtures for highway engineering[S]. Beijing: China Communications Press, 2011. (in Chinese)
[23] Ministry of Communications of the People's Republic of China. JTG E42—2005 Test methods of aggregate for highway engineering[S]. Beijing: China Communications Press, 2005. (in Chinese)

基于离散元的粗集料静压过程的迁移与演化规律

刘卫东　高　英

(东南大学交通学院, 南京 210096)

摘要:为研究粗集料在静止压实过程中的迁移与演化规律,基于离散单元法用不规则的多面体颗粒表示真实集料的形态特征,建立了由粗集料、空隙构成的数字试件,同时,建立了由数字试件及3块板构成的静止压实模型.以平均接触力、轴向应力、空隙率及配位数为评价指标,模拟压实位移为7.5,15与30 mm时粗集料在压实过程中的运动规律,并通过室内试验验证了此模型的可靠性.结果表明:轴向应力、平均接触力随着加载的进行,数值逐渐增加,压实位移与轴向应力、平均接触力正相关;不同压实位移的空隙率随着压实的进行不断减小,而配位数逐渐增大;总体上轴向应力、平均接触力、空隙率和配位数等4个指标在不同压实位移情况下变化幅度不同.研究结果为深入分析颗粒材料如沥青混合料或级配碎石的压实机理提供了一种方法.

关键词:沥青混合料;粗集料;静止压实;离散元模型
中图分类号:TU414